J. Mech. Phys. Solids Vol. 28, pp. 221–245
© Pergamon Press Ltd. 1980. Printed in Great Britain

0022-5096/80/1001-0221 $02.00/0

BIFURCATION PHENOMENA IN PURE BENDING

N. TRIANTAFYLLIDIS
Division of Engineering, Brown University, Providence, RI 02912, U.S.A.

(*Received* 18 *September* 1979)

ABSTRACT

THE BIFURCATION problem of an incompressible plate under pure bending is studied. Two incrementally linear constitutive models are employed. A classification of regimes of the bifurcation equation is also performed. An asymptotic analysis is carried out to establish the critical condition for short wavelength surface modes. Finally, a numerical calculation shows that in all cases considered the short wavelength surface mode in the compressive zone is the first bifurcation mode encountered in the deformation history.

1. INTRODUCTION

A STANDARD bifurcation problem is formulated for an incompressible plate, deforming in plane strain, subjected to pure bending. The motivation for this work stems from problems encountered in cold forming processes of metal sheets. More specifically, we are interested in investigating whether the onset of a bifurcation instability sets limits to the maximum curvature that can be attained in a ductile metal sheet by pure bending.

Two incrementally linear constitutive models are employed. One is the finite strain version of the simplest deformation theory of plasticity, introduced by STÖREN and RICE (1975), which is a hypoelastic constitutive law. The other is a path-independent non-linear elastic constitutive law. For both constitutive models the same uniaxial stress–strain behavior, described by a piecewise power law, is assumed.

The motivation for using these two constitutive models, arises from the desire to incorporate, in an approximate way, the destabilizing effect of a vertex on the current yield surface. We note that the models employed here are not proper plasticity laws, since no unloading is permitted. For a proper plasticity law, as will be discussed subsequently, unloading would precede the onset of bifurcation.

We begin by deriving the prebifurcation solution for pure bending of the plate. Both constitutive laws employed here give rise to the same prebifurcation solution. After briefly discussing the general formulation for the bifurcation problem of an incrementally linear solid, we formulate the eigenvalue problem governing bifurcation. Next, following the classification scheme introduced by HILL and HUTCHINSON (1975) the ranges of material properties for which the governing equation is in the elliptic, parabolic or hyperbolic regime are identified. Here we have the possibility of more than one regime coexisting, in different parts of the plate, at a

given stage of deformation since the prebifurcation stress state is a function of position in the body. For the same reason the characteristic lines are curves.

An asymptotic analysis is carried out for modes whose wavelength tends to zero. It is found that these are surface modes with critical condition identical to the ones given by HILL and HUTCHINSON (1975) and YOUNG (1976) for the plane strain half-space problem in tension and compression, respectively.

Finally, a finite element calculation shows that in all cases considered, the short wavelength surface bifurcation in the compressive zone occurs first and always before the maximum moment is attained.

2. PREBIFURCATION STATE

We consider an incompressible, isotropic, elastic plate whose cross-section in the unstressed state is a rectangle of length l_0 and height h_0. The solution will be carried out within the framework of the plane strain theory.

Although the pure bending (flexure) problem for such a rectangle has been solved, for a general hyperelastic material by RIVLIN (1950) (see also GREEN and ZERNA (1954)), for reasons of completeness we rederive the basic equations which will be needed in the subsequent analysis.

In view of the pure bending and the isotropy, the prebifurcation configuration is a portion of a cylinder and therefore cylindrical coordinates will be employed. At any point, the principal directions of strain (and stress) are radial and tangential and their corresponding principal values will carry subscripts 1 and 2 respectively.

Let $\bar{\kappa}$ be the curvature of the unstretched fiber, parallel to the traction-free surfaces, whose current (and original) length is l_0, as shown in Fig. 1. The stretch ratios of a material point at distance r from the axis of the cylinder are

$$\lambda_1 = \frac{1}{r\bar{\kappa}}, \qquad \lambda_2 = r\bar{\kappa}. \tag{2.1}$$

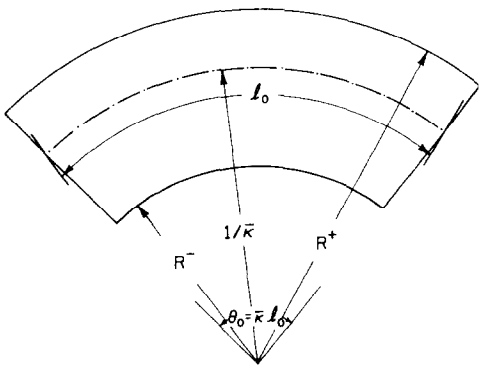

FIG. 1. Cross-section of the plate when the curvature of the currently unstretched fiber is $\bar{\kappa}$.

Thus the principal values of the logarithmic strain tensor are

$$\varepsilon_\alpha = \ln \lambda_\alpha.\dagger \tag{2.2}$$

For an incompressible isotropic material, whose complementary energy density function depends only on J_2, the second invariant of the Cauchy stress tensor, the constitutive equation can be put in the form

$$\varepsilon_i = \frac{\sigma_i'}{\frac{2}{3}E_s}, \tag{2.3}$$

where σ_i' is the ith principal value of the Cauchy stress deviator and E_s is the secant modulus of the uniaxial true stress σ vs natural strain ε curve at a stress level σ_e, with the equivalent stress σ_e given by

$$\sigma_e^2 = 3J_2 = \tfrac{3}{2}(\sigma_i'\sigma_i'). \tag{2.4}$$

The plane strain constraint $\varepsilon_3 = 0$ and the constitutive relation (2.3) give the lateral stress σ_3 as

$$\sigma_3 = \frac{\sigma_1 + \sigma_2}{2}, \tag{2.5}$$

and therefore, from (2.4) and (2.5), the equivalent stress σ_e can be written as

$$\sigma_e = \frac{\sqrt{3}}{2}|\sigma_1 - \sigma_2|. \tag{2.6}$$

We assume that the uniaxial stress–strain behavior is the following piecewise power law:

$$\varepsilon = \begin{cases} \dfrac{\sigma}{E} & \text{for } \sigma \leqslant \sigma_y, \\ \dfrac{\sigma_y}{E}\left(\dfrac{\sigma}{\sigma_y}\right)^m & \text{for } \sigma \geqslant \sigma_y, \end{cases} \tag{2.7}$$

where E is Young's modulus, m is the hardening exponent, and σ_y is the uniaxial yield stress.

From (2.7), the secant modulus E_s is found to be

$$E_s = \begin{cases} E & \text{for } \sigma_e \leqslant \sigma_y, \\ E\left(\dfrac{\sigma_e}{\sigma_y}\right)^{1-m} & \text{for } \sigma_e \geqslant \sigma_y. \end{cases} \tag{2.8}$$

Since the stress state is a function of r only, the only non-trivial equilibrium equation is

$$\frac{d\sigma_1}{dr} + \frac{\sigma_1 - \sigma_2}{r} = 0. \tag{2.9}$$

† Here and subsequently, Greek indices range from 1 to 2; Latin indices will range from 1 to 3 where 3 designates the third (out of plane) principal direction.

Employing (2.2), (2.3), (2.6) and (2.8) in (2.9) we obtain

$$\ln \bar{\kappa} r = \frac{3\tau_y}{2E}\left[r \frac{d}{dr}(\sigma_1/2\tau_y)\right]^{\chi} = \frac{3\tau_y}{2E}\left[\frac{d(\sigma_1/2\tau_y)}{d(\ln \bar{\kappa} r)}\right]^{\chi} \tag{2.10}$$

with

$$\chi = 1 \text{ for } |\sigma_1 - \sigma_2| \leqslant 2\tau_y \quad \text{and} \quad \chi = m \text{ for } |\sigma_1 - \sigma_2| \geqslant 2\tau_y$$

where

$$\tau_y = \frac{\sigma_y}{\sqrt{3}}$$

is the yield stress in simple shear. Upon integration, (2.10) yields

$$\left.\begin{aligned} \frac{\sigma_1}{2\tau_y} &= \frac{m}{m+1}\frac{3\tau_y}{2E}\left|\frac{2E}{3\tau_y}\ln \bar{\kappa} r\right|^{\frac{1}{m}+1} + c, \quad \text{for } |\ln \bar{\kappa} r| \geqslant \frac{3\tau_y}{2E}, \\ \frac{\sigma_1}{2\tau_y} &= \frac{1}{2}\frac{3\tau_y}{2E}\left|\frac{2E}{3\tau_y}\ln \bar{\kappa} r\right|^2 + c', \qquad \text{for } |\ln \bar{\kappa} r| \leqslant \frac{3\tau_y}{2E}, \end{aligned}\right\} \tag{2.11}$$

where c and c' are integration constants to be determined from the boundary conditions.

Let R^+ denote the radius, in the current configuration, of the outer fiber under tension and R^- the radius of the outer fiber under compression as shown in Fig. 1. From continuity of σ_1 and (2.11), we deduce that σ_1 must be an even function of $\ln \bar{\kappa} r$ and since σ_1 vanishes at both the free surfaces of the plate, we have

$$\bar{\kappa} R^+ = \frac{1}{\bar{\kappa} R^-}. \tag{2.12}$$

Incompressibility provides a second relation between R^+ and R^-, namely

$$(R^+)^2 - (R^-)^2 = \frac{2h_0}{\bar{\kappa}}, \tag{2.13}$$

which enables the radii of the outer fibers to be written as

$$\left.\begin{aligned} R^+ &= \frac{1}{\bar{\kappa}}\{\bar{\kappa} h_0 + [(\bar{\kappa} h_0)^2 + 1]^{\frac{1}{2}}\}^{\frac{1}{2}}, \\ R^- &= \frac{1}{\bar{\kappa}}\{[(\bar{\kappa} h_0)^2 + 1]^{\frac{1}{2}} - \bar{\kappa} h_0\}^{\frac{1}{2}}. \end{aligned}\right\} \tag{2.14}$$

Continuity of σ_1 as well as the traction-free boundary conditions completely specify the integration constants in (2.11) and therefore the prebifurcation stress field can be expressed in terms of the curvature of the currently unstretched fiber, $\bar{\kappa}$, the material properties (E, σ_y, m) and the initial plate thickness (h_0) as follows:

$$\left.\begin{aligned} \frac{\sigma_1}{2\tau_y} &= \frac{2E}{3\tau_y}\tfrac{1}{2}(\ln \bar{\kappa} r)^2 + \frac{1}{2}\frac{m-1}{m+1}\frac{3\tau_y}{2E} - \frac{m}{m+1}\left(\frac{2E}{3\tau_y}\right)^{\frac{1}{m}}(\ln \bar{\kappa} R^+)^{\frac{1}{m}+1}, \\ \frac{\sigma_2}{2\tau_y} &= \frac{2E}{3\tau_y}[\ln \bar{\kappa} r + \tfrac{1}{2}(\ln \bar{\kappa} r)^2] + \frac{1}{2}\frac{m-1}{m+1}\frac{3\tau_y}{2E} - \frac{m}{m+1}\left(\frac{2E}{3\tau_y}\right)^{\frac{1}{m}}(\ln \bar{\kappa} R^+)^{\frac{1}{m}+1}, \end{aligned}\right\} \tag{2.15}_1$$

for

$$\frac{1}{\bar{\kappa}}\exp\left(\frac{3\tau_y}{2E}\right) \geqslant r \geqslant \frac{1}{\bar{\kappa}}\exp\left(-\frac{3\tau_y}{2E}\right) \text{ (linear region)},$$

$$\left.\begin{aligned}
\frac{\sigma_1}{2\tau_y} &= \frac{m}{m+1}\left(\frac{2E}{3\tau_y}\right)^{\frac{1}{m}}\left[|\ln \bar{\kappa}r|^{\frac{1}{m}+1} - (\ln \bar{\kappa}R^+)^{\frac{1}{m}+1}\right], \\
\frac{\sigma_2}{2\tau_y} &= \left(\frac{2E}{3\tau_y}\right)^{\frac{1}{m}}\left\{|\ln \bar{\kappa}r|^{\frac{1}{m}} \operatorname{sgn}(\ln \bar{\kappa}r)\right. \\
&\qquad \left. + \frac{m}{m+1}\left[|\ln \bar{\kappa}r|^{\frac{1}{m}+1} - (\ln \bar{\kappa}R^+)^{\frac{1}{m}+1}\right]\right\},
\end{aligned}\right\} \quad (2.15)_2$$

for

$$R^+ \geqslant r \geqslant \frac{1}{\bar{\kappa}}\exp\left(\frac{3\tau_y}{2E}\right) \quad \text{or} \quad \frac{1}{\bar{\kappa}}\exp\left(-\frac{3\tau_y}{2E}\right) \geqslant r \geqslant R^- \text{ (nonlinear region)}.$$

A minimum requirement for the above solution to be a possible one for an elastic–plastic plate is that at each stage of the deformation history no strain-rate reversal occurs in the region of the plate that is currently under plastic loading.

Assuming that the loading criterion that must be satisfied throughout the current plastic region is

$$\sigma_i' \dot{\varepsilon}_i \geqslant 0, \tag{2.16}$$

and employing (2.2) and (2.15), (2.16) reduces to

$$\operatorname{sgn}(\ln \bar{\kappa}r)\left[\frac{\dot{\bar{\kappa}}}{\bar{\kappa}} + \frac{\dot{r}}{r}\right] \geqslant 0. \tag{2.17}$$

From incompressibility, the following relation between r and $\bar{\kappa}$, analogous to (2.13) is obtained

$$(R^+)^2 - r^2 = \frac{2f_0}{\bar{\kappa}}, \tag{2.18}$$

where f_0 is the distance in the unstressed configuration between the two fibers with current radii R^+ and r. Using the incremental form of (2.18), (2.17) can be put in the form

$$\operatorname{sgn}(\ln \bar{\kappa}r)\frac{\dot{\bar{\kappa}}}{\bar{\kappa}}\left[1 - \frac{1}{(\bar{\kappa}r)^2\sqrt{1+(\bar{\kappa}h_0)^2}}\right] \geqslant 0, \tag{2.19}$$

and thus we deduce that unloading is possible in part of the plate if

$$\bar{\kappa}h_0 > \sqrt{\exp(6\tau_y/E) - 1} = \sqrt{\exp(2\sqrt{3}\sigma_y/E) - 1}. \tag{2.20}$$

For structural metals, σ_y/E is within the range from 0·001 to 0·01. For $\sigma_y/E = 0{\cdot}001$, unloading will start as soon as $\bar{\kappa}$ exceeds $0{\cdot}059/h_0$; and in the case of $\sigma_y/E = 0{\cdot}01$, unloading begins at $\bar{\kappa} = 0{\cdot}188/h_0$ which is still small compared to the expected critical curvatures at bifurcation. Consequently, we anticipate that the prebifurcation

solution for an elastic-plastic material with a uniaxial curve given by (2.7) will differ from (2.15) due to the presence of unloading.

3. BIFURCATION ANALYSIS

3.1 *General formulation*

A Lagrangian formulation of the field equations is adopted. Material points in the body of volume V and surface S in the undeformed configuration are identified by a set of convected coordinates x^i and the covariant components of the metric tensor in the undeformed body are denoted by g_{ij}. Also let u_i be the covariant components of the displacement vector with respect to the undeformed basis. Moreover $\dot{(\cdot)}$ denotes the derivative of $(\cdot)$ with respect to some monotonically increasing parameter, which is also referred to as an increment of the quantity in question and by a comma we denote the covariant differentiation with respect to the undeformed body's metric.

The prebifurcation state of the body can be completely specified as a function of the scalar quantity $\bar{\kappa}$ as discussed in the previous Section 2. All quantities associated with the fundamental solution whose uniqueness is in question are labeled by a superscript or subscript 0. The fundamental solution starts at $\bar{\kappa} = 0$ and is associated with monotonically increasing $\bar{\kappa}$.

At some stage of deformation, suppose that bifurcation is possible, so that for a given increment $\dot{\bar{\kappa}}$ there exist two different solutions $\dot{u}_i^\alpha$ and $\dot{u}_i^\beta$. Introduce the following notation for the difference between two possible solutions α and β in any field quantity:

$$\Delta(\cdot) = (\cdot)^\beta - (\cdot)^\alpha. \tag{3.1}$$

If T^i are the contravariant components of the nominal traction vector at the surface of the body, with respect to the undeformed basis, then at bifurcation $\dot{T}^i = 0$ or $\dot{u}_i = 0$ in these parts of the surface where the traction or the displacement increments are respectively prescribed, and since both solutions α and β satisfy the equilibrium equations, the principle of virtual work gives (HILL, 1957)

$$0 = \int_S \Delta\dot{T}^i \Delta\dot{u}_i \, dS = \int_V (\Delta\dot{\tau}^{ij}\Delta\dot{E}_{ij} + \tau_0^{ij}\Delta\dot{u}_{k,i}\Delta\dot{u}^k_{,j}) \, dV, \tag{3.2}$$

where E_{ij} denotes the covariant components of the Green strain tensor, τ^{ij} the covariant components of the Kirchhoff stress and $\dot{\tau}^{ij}$ are the covariant components of its convected derivative. $\Delta\dot{E}_{ij}$ can be expressed in terms of $\Delta\dot{u}_i$ as follows:

$$\Delta\dot{E}_{ij} = \tfrac{1}{2}(\Delta\dot{u}_{i,j} + \Delta\dot{u}_{j,i}) + \tfrac{1}{2}(\dot{u}^k_{,i}\Delta\dot{u}_{k,j} + \dot{u}^k_{,j}\Delta\dot{u}_{k,i}). \tag{3.3}$$

In this paper attention is focused on incrementally linear, incompressible solids obeying the general constitutive equation

$$\overset{\nabla}{\tau}{}^{ij} = \overset{\nabla}{\sigma}{}^{ij} = C^{ijkl}\dot{E}_{kl} - \dot{p}G^{ij}, \tag{3.4}$$

where $\overset{\nabla}{\sigma}{}^{ij}$ are the contravariant components of the Jaumann derivative of the Cauchy stress, $\dot{p}$ the hydrostatic pressure increment, G^{ij} the current metric tensor's components and C^{ijkl} the moduli, which are functions of the material properties and the current state. Equation (3.4) can be transformed equivalently to a relation

involving the convected derivative of Kirchhoff stress:

$$\dot{\tau}^{ij} = L^{ijkl}\dot{E}_{kl} - \dot{p}G^{ij}, \tag{3.5}$$

where

$$L^{ijkl} = C^{ijkl} - \tfrac{1}{2}(G^{ik}\sigma^{jl} + G^{jk}\sigma^{il} + G^{il}\sigma^{jk} + G^{jl}\sigma^{ik}). \tag{3.6}$$

The moduli C^{ijkl} are taken to satisfy the symmetry $C^{ijkl} = C^{klij}$ in addition to the trivial ones $C^{ijkl} = C^{jikl} = C^{ijlk}$. By inspection, the same symmetries are exhibited by L^{ijkl}.

Making use of the constitutive law (3.5) in (3.2), bifurcation is excluded when the functional F defined as (HILL, 1957)

$$F[\bar{\kappa}, \Delta\dot{u}_i] \equiv \int_V (L^{ijkl}\Delta\dot{E}_{ij}\Delta\dot{E}_{kl} + \tau_0^{ij}\Delta\dot{u}_{k,i}\Delta\dot{u}^k_{,j})\, dV \tag{3.7}$$

is positive definite. A bifurcation mode $\overset{(1)}{u}_i$ satisfies (see, for instance, HILL (1957))

$$F[\bar{\kappa}_{cr}, \overset{(1)}{u}_i] = 0, \qquad \delta F[\bar{\kappa}_{cr}, \overset{(1)}{u}_i] = 0 \tag{3.8}$$

subject to the boundary condition $\overset{(1)}{u}_i = 0$ on the part of the surface where the displacement increments are specified. In addition, for an incompressible material, $\overset{(1)}{u}_i$ satisfies the constraint

$$G^{ij}\overset{(1)}{u}{}^k_{,i}\overset{(1)}{u}_{kj} + \overset{(1)}{u}{}^i_{,i} = 0.$$

3.2 *Problem formulation*

Here, for simplicity, the current configuration is taken to be the reference one and therefore, as in Section 2, cylindrical coordinates are employed with $x^1 = r$, $x^2 = \theta$, $x^3 = z$.

In the case of plane strain and for an incompressible material, the bifurcation functional F in (3.7) assumes the form

$$F[\bar{\kappa}, \Delta\dot{u}_\alpha] = \int_0^{\bar{\kappa}l_0}\int_{R^-}^{R^+} \{L_{\alpha\beta\gamma\delta}\Delta\dot{E}_{\alpha\beta}\Delta\dot{E}_{\gamma\delta} + \sigma_{\alpha\beta}\Delta\dot{u}_{\mu,\alpha}\Delta\dot{u}_{\mu,\beta}\}\, r\, dr\, d\theta\,, \tag{3.9}$$

where physical components of tensors are employed. The physical components of $\Delta\dot{u}_{i,j}$ in cylindrical coordinates are

$$\left.\begin{aligned} \Delta\dot{u}_{1,1} &= \frac{\partial\Delta\dot{u}_1}{\partial r}, \qquad \Delta\dot{u}_{1,2} = \frac{1}{r}\frac{\partial\Delta\dot{u}_1}{\partial\theta} - \frac{\Delta\dot{u}_2}{r}, \\ \Delta\dot{u}_{2,1} &= \frac{\partial\Delta\dot{u}_2}{\partial r}, \qquad \Delta\dot{u}_{2,2} = \frac{1}{r}\frac{\partial\Delta\dot{u}_2}{\partial\theta} + \frac{\Delta\dot{u}_1}{r}. \end{aligned}\right\} \tag{3.10}$$

Incompressibility implies

$$\frac{\partial}{\partial r}(r\,\Delta\dot{u}_1) + \frac{\partial\,\Delta\dot{u}_2}{\partial\theta} = 0, \tag{3.11}$$

and thus there exists a potential function $\Phi(r, \theta)$ such that

$$\Delta\dot{u}_1 = -\frac{1}{r}\frac{\partial\Phi}{\partial\theta}, \qquad \Delta\dot{u}_2 = \frac{\partial\Phi}{\partial r}. \tag{3.12}$$

Two incrementally linear constitutive models are used in this analysis. The choice of these two constitutive laws is motivated from the desire to incorporate, in a rather simple way, the destabilizing effect of a vertex on the current yield surface of the solid.

It has been observed that (see HUTCHINSON (1974)) bifurcation predictions based on flow theory with a smooth yield surface, consistently over-estimate the bifurcation stresses. Analytical studies of polycrystalline aggregates predict the formation of a corner in the yield surface (HILL, 1967; HUTCHINSON, 1970; LIN, 1971). Of particular relevance here is that, after tensile straining into the plastic range, the incremental shear moduli are greatly reduced from their elastic value. Experimental evidence, in spite of the abundance of experiments, is not conclusive (HECKER, 1976).

A simple way to approximate the destabilizing effect of a corner at the yield surface is to use deformation theories of plasticity and among them the J_2 deformation theory is the most frequently used for bifurcation calculations at small strain levels.

In the case of large strain there is no unique generalization of the J_2 deformation theory. Here two different such generalizations will be considered: the finite strain version proposed by STÖREN and RICE (1975), which is a hypoelastic model since no strain energy density function exists, and the hyperelastic model, both with the same uniaxial stress–strain curve (2.7).

The prebifurcation solution for both constitutive laws is given by (2.15) since in our case the principal axes of the material strain ellipsoid are fixed with respect to the material, and thus, as discussed by STÖREN and RICE (1975), path-independence holds for their hypoelastic model. In the two constitutive theories employed, only the corresponding incremental shear moduli differ (more specifically; the hyperelastic incremental shear modulus is always greater, for a given stress level, than the hypoelastic one). This difference, negligible for small strains, can be substantial at large strains and, as we shall see, it may under certain circumstances affect significantly the type of bifurcation predicted. For a detailed discussion of the justification of the use of deformation theories in bifurcation analyses of elastic–plastic solids see HUTCHINSON (1974).

The contravariant components of the incremental moduli tensor C^{ijkl} for the incompressible hypoelastic material of STÖREN and RICE (1975) are

$$C^{ijkl} = \bar{h}\left[\tfrac{1}{2}(g^{ik}g^{jl}+g^{jk}g^{il}) - \frac{3}{2}\left(1-\frac{h}{\bar{h}}\right)\frac{\sigma'^{ij}\sigma'^{kl}}{\sigma_e^2}\right], \tag{3.13}$$

where $\bar{h} = \frac{2}{3}E_s$, $h = \frac{2}{3}E_t$ and σ'^{ij} are the contravariant components of the Cauchy stress deviator with E_s and E_t, respectively, the secant and tangent moduli at stress-level σ_e. For the piecewise power law (2.7) adopted in this analysis, E_s is given by (2.8) and the tangent modulus E_t by

$$E_t = \begin{cases} E & \text{for } \sigma_e \leqslant \sigma_y, \\ \dfrac{E}{m}\left(\dfrac{\sigma_e}{\sigma_y}\right)^{1-m} & \text{for } \sigma_e > \sigma_y. \end{cases} \tag{3.14}$$

Therefore, for the hypoelastic model, (3.13), with the help of (3.6), yields the following expressions for the non-vanishing physical components of the incremental moduli

tensor $\mathbf{L}$:

$$\left.\begin{aligned} L_{1111} &= \frac{\bar{h}}{2}\left(1+\frac{h}{\bar{h}}\right)-2\sigma_1, \qquad L_{1122}=L_{2211}=\frac{\bar{h}}{2}\left(1-\frac{h}{\bar{h}}\right), \\ L_{2222} &= \frac{\bar{h}}{2}\left(1+\frac{h}{\bar{h}}\right)-2\sigma_2, \end{aligned}\right\} \tag{3.15}$$

$$L_{1212}=L_{2112}=L_{2121}=L_{1221}=\frac{\bar{h}}{2}-\frac{\sigma_1+\sigma_2}{2}, \tag{3.16}$$

with σ_1, σ_2 given by (2.15).

For the hyperelastic constitutive law the normal incremental moduli are also calculated from (3.15). Since r and θ are the principal axes coordinates the incremental shear modulus is given by (BIOT, 1965; HILL, 1969)

$$L_{1212}^{\text{hyper}}=\frac{1}{2}\frac{\lambda_1^2+\lambda_2^2}{\lambda_1^2-\lambda_2^2}(\sigma_1-\sigma_2)-\frac{\sigma_1+\sigma_2}{2}=\frac{\bar{h}}{2}\left[\frac{(\bar{\kappa}r)^4+1}{(\bar{\kappa}r)^4-1}\cdot 2\ln\bar{\kappa}r\right]-\frac{\sigma_1+\sigma_2}{2}, \tag{3.17}$$

where for the second equation we used (2.1) and (2.15). Note that for small strain (that is, $\bar{\kappa}r\to 1$), the quantity in brackets in (3.17) converges to unity and thus in this limit the moduli in (3.16) and (3.17) coincide.

In view of (3.12) the bifurcation functional F in (3.9) can be expressed as a functional of the velocity potential Φ. With the help of (3.10), (3.15), (3.16) and (3.17) in (3.9) we find that

$$F[\bar{\kappa},\Phi]=\int_0^{\bar{\kappa}l_0}\int_{R^-}^{R^+}\left[(2h-\sigma_1-\sigma_2)\left(\frac{1}{r^2}\frac{\partial\Phi}{\partial\theta}-\frac{1}{r}\frac{\partial^2\Phi}{\partial r\,\partial\theta}\right)^2+\tfrac{1}{2}(\gamma\bar{h}-\sigma_1-\sigma_2)\right.$$

$$\left.\times\left(-\frac{1}{r^2}\frac{\partial^2\Phi}{\partial\theta^2}+\frac{\partial^2\Phi}{\partial r^2}-\frac{1}{r}\frac{\partial\Phi}{\partial r}\right)^2+\sigma_1\left(\frac{\partial^2\Phi}{\partial r^2}\right)^2+\sigma_2\left(\frac{1}{r^2}\frac{\partial^2\Phi}{\partial\theta^2}+\frac{1}{r}\frac{\partial\Phi}{\partial r}\right)^2\right]r\,dr\,d\theta, \tag{3.18}$$

with

$$\gamma=\left\{\begin{aligned} &1 \text{ for the hypoelastic model,} \\ &2\,(\ln\bar{\kappa}r)\frac{(\bar{\kappa}r)^4+1}{(\bar{\kappa}r)^4-1} \text{ for the hyperelastic model.}\end{aligned}\right\} \tag{3.19}$$

The bifurcation problem is solved for two different sets of boundary conditions in order to take into account, in an approximate way, the stiffness of the loading device.

First we consider the case when the moment at both the ends of the plate is actually controlled during the deformation process (loading machine with negligible stiffness). The corresponding boundary condition is

$$\Delta\dot{T}_1=\Delta\dot{T}_2=0 \quad \text{for } \theta=0,\bar{\kappa}l_0, \tag{3.20}$$

with $\dot{T}_1, \dot{T}_2$ the physical components of the nominal traction increment.

In the second case we assume that the relative rotation of the ends of the plate is prescribed and that the end sections remain always plane and cannot sustain any

shear traction (very stiff machine). The analytical expression of these requirements is

$$\Delta\dot{u}_2 = 0 \quad \text{and} \quad \Delta\dot{T}_1 = 0 \quad \text{for } \theta = 0, \bar{\kappa} l_0. \tag{3.21}$$

In addition to (3.20) or (3.21), since the top and bottom surfaces of the plate are traction free the following boundary conditions must be satisfied, in both cases:

$$\Delta\dot{T}_1 = \Delta\dot{T}_2 = 0 \quad \text{for } r = R^-, R^+. \tag{3.22}$$

For the boundary conditions (3.20) and (3.22) any admissible potential function Φ can be represented as

$$\Phi(r, \theta) = \phi_{co}(r) + \sum_{n=1}^{\infty} \left[\phi_{cn}(r) \cos\left(\frac{2\pi n\theta}{\bar{\kappa} l_0}\right) + \phi_{sn}(r) \sin\left(\frac{2\pi n\theta}{\bar{\kappa} l_0}\right)\right], \tag{3.23}$$

with $n = 1, 2, 3, \ldots$, and $\phi_{cn}(r)$, $\phi_{sn}(r)$ any continuously differentiable functions of r.

For the boundary conditions (3.21) and (3.22) the potential Φ assumes the form

$$\Phi(r, \theta) = \sum_{n=1}^{\infty} \left\{ \phi_{cn}(r) \left[\cos\left(\frac{2\pi n\theta}{\bar{\kappa} l_0}\right) - 1 \right] + \phi_{sn}(r) \sin\left(\frac{2\pi n\theta}{\bar{\kappa} l_0}\right)\right\}, \tag{3.24}$$

where again $\phi_{cn}(r)$, $\phi_{sn}(r)$ are arbitrary continuously differentiable functions of r, and upon successive substitution of (3.23) and (3.24) in (3.18), in view of the orthogonality of the trigonometric functions the bifurcation functional F becomes

$$F[\bar{\kappa}, \Phi] = F_0[\bar{\kappa}, \phi_{co}] + \frac{1}{2} \sum_{n=1}^{\infty} (F_n[\bar{\kappa}, \phi_{sn}] + F_n[\bar{\kappa}, \phi_{cn}]) \tag{3.25}$$

when the moment at the ends is prescribed (boundary conditions (3.20) and (3.22)), and

$$F[\bar{\kappa}, \Phi] = F_0\left[\bar{\kappa}, \sum_{n=1}^{\infty} \phi_{cn}\right] + \frac{1}{2} \sum_{n=1}^{\infty} (F_n[\bar{\kappa}, \phi_{sn}] + F_n[\bar{\kappa}, \phi_{cn}]) \tag{3.26}$$

in the case of prescribed relative end rotation (boundary conditions (3.21) and (3.22)). In (3.25) and (3.26), F_n is given by

$$\begin{aligned} F_n[\bar{\kappa}, \phi] = \int_{R^-}^{R^+} \Bigg\{ & (2h - \sigma_1 - \sigma_2) \left(\left[\frac{2\pi n}{\bar{\kappa} l_0}\right] \frac{\phi}{r^2} - \left[\frac{2\pi n}{\bar{\kappa} l_0}\right] \frac{1}{r} \frac{d\phi}{dr} \right)^2 \\ & + \tfrac{1}{2}(\gamma\bar{h} - \sigma_1 - \sigma_2) \left(\left[\frac{2\pi n}{\bar{\kappa} l_0}\right]^2 \frac{\phi}{r^2} + \frac{d^2\phi}{dr^2} - \frac{1}{r} \frac{d\phi}{dr} \right)^2 \\ & + \sigma_1 \left(\frac{d^2\phi}{dr^2} \right)^2 + \sigma_2 \left(\left[\frac{2\pi n}{\bar{\kappa} l_0}\right]^2 \frac{\phi}{r^2} - \frac{1}{r} \frac{d\phi}{dr} \right)^2 \Bigg\} r\, dr \quad (n = 1, 2, 3, \ldots). \end{aligned} \tag{3.27}$$

The critical curvature at the first bifurcation is then given by the minimum, over all integers n, of the lowest eigenvalue of each functional F_n. The corresponding eigenmodes are of the form $\phi(r) \cos(2\pi n\theta/\bar{\kappa} l_0)$ or $\phi(r) \sin(2\pi n\theta/\bar{\kappa} l_0)$ for (3.25) and $\phi(r) \sin(2\pi n\theta/\bar{\kappa} l_0)$ for (3.26).

Of course we must ensure that none of the eigenmodes corresponds to rigid body motion and that the plate is not bent to an angle exceeding 360°. Using (3.10) and (3.12) both these requirements are satisfied for $n \neq 0$ as long as $\bar{\kappa} l_0 < 2\pi$.

3.3 *Classification of regimes*

Following HILL and HUTCHINSON (1975), the general character of the bifurcation equation is investigated, for materials obeying constitutive laws of the form (3.4). Specifically the range of curvature $\bar{\kappa}$ and the material properties for which this equation is elliptic, parabolic or hyperbolic are determined. The approach adopted here is a generalization of the results given in HILL and HUTCHINSON (1975) and YOUNG (1976) for the case of a non-uniform prebifurcation stress field.

The bifurcation equation, obtained from the variational principle (3.8) with the help of (3.18), is a fourth-order linear partial differential equation in the potential function $\Phi(r, \theta)$:

$$(\gamma\bar{h}+\sigma_1-\sigma_2)\frac{\partial^4\Phi}{\partial r^4}+2(2h-\gamma\bar{h})\frac{1}{r^2}\frac{\partial^4\Phi}{\partial r^2\,\partial\theta^2}+(\gamma\bar{h}-\sigma_1+\sigma_2)\frac{1}{r^4}\frac{\partial^4\Phi}{\partial\theta^4}+Q[\Phi]=0, \tag{3.28}$$

where γ is given by (3.19) and Q is a linear operator of third order whose exact form need not be specified here. If n_1 and n_2 are the physical components of the unit vector $\mathbf{n}$ which is normal to a characteristic of (3.28), they must satisfy the relation (see, for instance, HILBERT and COURANT (1953))

$$(\gamma\bar{h}+\sigma_1-\sigma_2)(n_1)^4+2(2h-\gamma\bar{h})(n_1n_2)^2+(\gamma\bar{h}-\sigma_1+\sigma_2)(n_2)^4=0. \tag{3.29}$$

When (3.29) admits real roots, we can construct a potential Φ that satisfies (3.28) and whose second derivatives are discontinuous across the characteristics. These solutions of the bifurcation equation will have jumps in the incremental stress and strain fields across the characteristic curves.

Alternatively, (3.29) could have been obtained as in HILL and HUTCHINSON (1975, Appendix AII), using the appropriate jump conditions for the strain and traction increments across the characteristics. We note that (3.29) is identical to the characteristic equation obtained by HILL and HUTCHINSON (1975) for the bifurcation problem of an incompressible rectangle, in plane strain, subject to uniform stress parallel to its traction-free surface. Since the characteristic direction at a given point depends only on its local stress state and observing that in both problems the principal stress coordinate system is used, this coincidence is expected. However, here the characteristic lines are curves, for the prebifurcation stress field is now a function of the position in the body.

In conformity with the standard nomenclature for systems of partial differential equations, a material point belongs to the elliptic, parabolic or hyperbolic regime, according to whether, at this point, (3.29) has no, two or four real roots, respectively. The classification of regimes is carried out for each of the constitutive models employed in this paper.

3.3.1 *Hypoelastic model.*

(i) Elliptic regime

For a point to be in the elliptic regime, (3.29) must have no real roots. This is

equivalent to

$$|\sigma_1-\sigma_2|<2h\sqrt{\frac{\gamma\bar{h}}{h}-1}$$

or

$$\gamma\bar{h}>|\sigma_1-\sigma_2|>2h\sqrt{\frac{\gamma\bar{h}}{h}-1}\quad\text{and}\quad 2h-\gamma\bar{h}>0. \tag{3.30}$$

Using (2.8), (2.15), (3.14) and (3.19) we obtain from (3.30),

$$\left.\begin{aligned}|\ln\bar{\kappa}r|&<\frac{\sqrt{m-1}}{m}\quad\text{for } m\geqslant 2,\\ |\ln\bar{\kappa}r|&<\tfrac{1}{2}\qquad\text{for } m\leqslant 2.\end{aligned}\right\} \tag{3.31}$$

The outer fibers, whose radii are given in (2.14), and thus the entire plate will be in the elliptic regime provided that

$$\left.\begin{aligned}\bar{\kappa}h_0&<\frac{\exp\left(\dfrac{4\sqrt{m-1}}{m}\right)-1}{2\exp\left(\dfrac{2\sqrt{m-1}}{m}\right)}\quad\text{for } m\geqslant 2,\\ \bar{\kappa}h_0&<\frac{e^2-1}{2e}\qquad\text{for } m\leqslant 2.\end{aligned}\right\} \tag{3.32}$$

(ii) Parabolic regime

For a point to be in the parabolic regime, the product of the roots of (3.29) must be negative, which implies

$$(\bar{\gamma}h)^2-(\sigma_1-\sigma_2)^2\leqslant 0. \tag{3.33}$$

Employing (2.8), (2.15) and (3.19), (3.33) can be rewritten as

$$|\ln\bar{\kappa}r|>\tfrac{1}{2}. \tag{3.34}$$

Therefore, part of the plate will be in the parabolic regime when

$$\ln\bar{\kappa}R^+>\tfrac{1}{2} \tag{3.35}$$

or equivalently from (2.14) if

$$\bar{\kappa}h_0>\frac{e^2-1}{2e}. \tag{3.36}$$

(iii) Hyperbolic regime

From (3.31) and (3.34), part of the plate is in the hyperbolic regime when

$$\bar{\kappa}h_0>\frac{\exp\left(\dfrac{4\sqrt{m-1}}{m}\right)-1}{2\exp\left(\dfrac{2\sqrt{m-1}}{m}\right)}\quad\text{for } m\geqslant 2. \tag{3.37}$$

For $m \leqslant 2$, the characteristic equation (3.29) has at most two real roots and hence it is impossible to have part of the plate in the hyperbolic region at any stage of deformation.

3.3.2 *Hyperelastic model.*

(i) Elliptic regime

For a point to be in the elliptic regime, (3.30) gives, making use of (2.8), (2.15), (3.14) and (3.19),

$$|m \ln \bar{\kappa} r|^2 - 2|m \ln \bar{\kappa} r| \left| \frac{(\bar{\kappa} r)^4 + 1}{(\bar{\kappa} r)^4 - 1} \right| + 1 < 0 \tag{3.38}_1$$

or

$$\frac{1}{m} > |\ln \bar{\kappa} r| \left| \frac{(\bar{\kappa} r)^4 + 1}{(\bar{\kappa} r)^4 - 1} \right| \quad \text{and} \quad |m \ln \bar{\kappa} r|^2 - 2|m \ln \bar{\kappa} r| \left| \frac{(\bar{\kappa} r)^4 + 1}{(\bar{\kappa} r)^4 - 1} \right| + 1 \geqslant 0. \tag{3.38}_2$$

The inequality $(3.38)_1$ is satisfied for $|m \ln \bar{\kappa} r|$ lying between the roots of the quadratic equation

$$x^2 - 2x \frac{(\bar{\kappa} r)^4 + 1}{|(\bar{\kappa} r)^4 - 1|} + 1 = 0,$$

and thus can be rewritten as

$$\left| \frac{(\bar{\kappa} r)^2 - 1}{(\bar{\kappa} r)^2 + 1} \right| < \frac{m}{2} |\ln (\bar{\kappa} r)^2| < \left| \frac{(\bar{\kappa} r)^2 + 1}{(\bar{\kappa} r)^2 - 1} \right|. \tag{3.39}$$

Taking into account (3.39), one can show that the two inequalities in $(3.38)_2$ are mutually exclusive. The left part of inequality (3.39) is an identity for $m > 1$. For the right part we observe that $\frac{1}{2} m \ln x - (x+1)/(x-1)$ is an increasing function of x for $m \geqslant 1$ and $x \geqslant 1$. Thus for the entire plate to be in the elliptic regime we must have

$$\frac{m}{2} \ln (\bar{\kappa} R^+)^2 < \frac{(\bar{\kappa} R^+)^2 + 1}{(\bar{\kappa} R^+)^2 - 1} \tag{3.40}$$

which, combined with (2.14), transforms to

$$\bar{\kappa} h_0 < \frac{\exp (4x_0(m)) - 1}{2 \exp (2x_0(m))}, \tag{3.41}$$

where $x_0(m)$ is the positive root of the equation

$$x \tanh x = \frac{1}{m}. \tag{3.42}$$

(ii) Parabolic regime

A straightforward calculation involving (3.33), (2.8), (2.15) and (3.19) shows that the characteristic equation (3.29) cannot have only two real roots and therefore the hyperelastic plate never enters the parabolic regime. This property, which characterizes incompressible finitely-elastic materials in plane strain, was noted by BIOT (1965) (cf. HILL and HUTCHINSON, 1975).

(iii) Hyperbolic regime

Combining the results obtained from the two previous cases, we conclude that for part of the plate to be in the hyperbolic regime,

$$\bar{\kappa}h_0 > \frac{\exp(4x_0(m)) - 1}{2\exp(2x_0(m))}, \tag{3.43}$$

where again $x_0(m)$ is the positive root of equation (3.42).

3.3.3 *Characteristics.*

From (3.29) the equation of the characteristics in polar coordinates is

$$\frac{n_1}{n_2} = -\frac{r\,d\theta}{dr} = \pm\sqrt{\frac{\gamma\bar{h} - 2h \pm \sqrt{(\gamma\bar{h}-2h)^2 - (\gamma\bar{h})^2 + (\sigma_2-\sigma_1)^2}}{\gamma\bar{h} - (\sigma_2-\sigma_1)}} \tag{3.44}$$

which, for the hypoelastic mode, yields

$$\theta = \pm\int\sqrt{\frac{1 - \frac{2}{m} + 2s\sqrt{\frac{1}{m^2} - \frac{1}{m} + x^2}}{1-2x}}\,dx, \tag{3.45}$$

and, for the hyperelastic one,

$$\theta = \pm\int\sqrt{\frac{e^{4x}-1}{2} - \frac{e^{4x}-1}{2mx} + s\frac{e^{4x}-1}{2x}\sqrt{\frac{1}{m^2} - \frac{2x}{m}\frac{e^{4x}+1}{e^{4x}-1} + x^2}}\,dx, \tag{3.46}$$

where in (3.45) and (3.46) $s = +1$ or -1 and $x = \ln \bar{\kappa}r$. Some representative characteristics are depicted in Figs 2 and 3 for a hypoelastic and a hyperelastic material, respectively. In both cases the hardening exponent, m, is 4 and the curvature, $\bar{\kappa}h_0$, is 2·80. Characteristics are labeled with an α or a β according to whether the parameter s in equations (3.45) and (3.46) takes the value $+1$ or -1.

In both figures the α- and β-lines have common tangents at points belonging to the elliptic–hyperbolic boundaries. We also note that in Fig. 2 (hypoelastic body) the

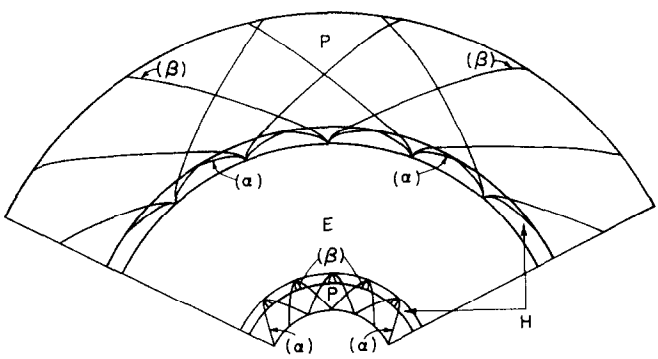

FIG. 2. Characteristic curves and regimes (E stands for elliptic, H for hyperbolic, P for parabolic) in a hypoelastic plate when $\bar{\kappa}h_0 = 2{\cdot}80$, $m = 4$, $\varepsilon_y = 0{\cdot}002$.

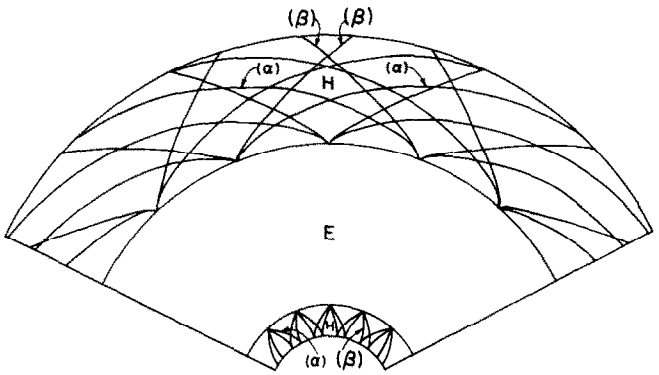

FIG. 3. Characteristic curves and regimes (E stands for elliptic, H for hyperbolic) in a hyperelastic plate when $\bar{\kappa}h_0 = 2{\cdot}80$, $m = 4$, $\varepsilon_y = 0{\cdot}002$.

α-lines are tangent to the hyperbolic–parabolic boundary in the tensile zone while the β-lines are perpendicular to the hyperbolic–parabolic boundary in the compressive zone.

A general property of the characteristics is that they never appear before the first bifurcation. This statement can be formalized in the following proposition. *If at some state, specified by the curvature $\bar{\kappa}^*$, part of the body is in the parabolic or in the hyperbolic regime, then there exists at least one bifurcation point with $\bar{\kappa}_{cr} \leqslant \bar{\kappa}^*$.* A similar proposition, stated by RICE (1976) was proved for the case of a homogeneous prebifurcation stress field, using a procedure introduced by VAN HOVE (1947).

To prove our assertion, it is enough to show that if for some $\bar{\kappa}^*$ part of the body is in the parabolic or hyperbolic regime, we can find a non-trivial potential function Φ, satisfying the essential boundary conditions, such that $F[\bar{\kappa}^*, \Phi] < 0$.

For this, consider $\Phi = \sin[\xi w(r, \theta)]$ where $w(r, \theta)$ is an adequately smooth, bounded function that vanishes for points which either lie in the elliptic regime or are very close to the boundary. For large ξ, the bifurcation functional F given by (3.18) takes the form

$$F[\bar{\kappa}^*, \sin(\xi w)] = \xi^4 \tfrac{1}{2} \int_0^{\bar{\kappa}^* l_0 R^+} \int_{R^-} \left\{ \left[(\gamma\bar{h} + \sigma_1 - \sigma_2) \left(\frac{\partial w}{\partial r} \right)^4 + 2(2h - \gamma\bar{h}) \left(\frac{1}{r} \frac{\partial w}{\partial \theta} \frac{\partial w}{\partial r} \right)^2 + (\gamma\bar{h} - \sigma_1 + \sigma_2) \left(\frac{1}{r} \frac{\partial w}{\partial \theta} \right)^4 \right] \sin^2(\xi w) \right\} r \, dr \, d\theta + O(\xi^3). \quad (3.47)$$

If part of the structure is in the parabolic or the hyperbolic regime, we can construct the function w to satisfy the additional property

$$\frac{1}{r} \frac{\partial w}{\partial \theta} \Big/ \frac{\partial w}{\partial r} = [(\gamma\bar{h} - 2h)/(\gamma\bar{h} - \sigma_1 + \sigma_2)]^{\frac{1}{2}} \quad (3.48)$$

for points in the hyperbolic regime or

$$\frac{\partial w}{\partial \theta} = 0 \quad (3.49)$$

for points in the parabolic regime. This construction ensures that the integrand in the dominant term of (3.47) is negative and thus, for large enough ξ, the bifurcation functional F is also negative.

This property of the characteristics actually holds more generally for an incrementally linear material that satisfies normality, given that the bifurcation functional is adequately smooth with respect to the monotonically increasing loading parameter. The proof in the general case is similar to the one outlined above.

3.4 *The short wavelength limit*

As we have seen in Section 3.2 the eigenmodes have the form $\phi(r)\cos[2\pi n\theta/\bar{\kappa}l_0]$ or $\phi(r)\sin[2\pi n\theta/\bar{\kappa}l_0]$. For the short wavelength limit $n\to\infty$ the critical curvature as well as the asymptotic form of the eigenmode can be calculated analytically.

The variational form of the bifurcation equation corresponding to wavenumber n is $\delta F_n = 0$, where F_n is given by (3.27). Using the substitution $x = \ln \bar{\kappa}r$, the resulting Euler equation is

$$[n^4(\gamma\bar{h}-\sigma_1+\sigma_2)+O(n^2)]\phi+O(n^2)\frac{d\phi}{dx}+[2n^2(\gamma\bar{h}-2h)+O(1)]\frac{d^2\phi}{dx^2}$$
$$+O(1)\frac{d^3\phi}{dx^3}+[\gamma\bar{h}+\sigma_1-\sigma_2]\frac{d^4\phi}{dx^4}=0, \tag{3.50}$$

together with the traction-free boundary conditions

$$\left.\begin{aligned}&[n^2(\gamma\bar{h}-\sigma_1-\sigma_2)]\phi+O(1)\frac{d\phi}{dx}+(\gamma\bar{h}+\sigma_1-\sigma_2)\frac{d^2\phi}{dx^2}=0,\\ &O(n^2)\phi+[n^2(-4h+\gamma\bar{h}+\sigma_1+\sigma_2)+O(1)]\frac{d\phi}{dx}+O(1)\frac{d^2\phi}{dx^2}\\ &\qquad+[\gamma\bar{h}+\sigma_1-\sigma_2]\frac{d^3\phi}{dx^3}=0,\end{aligned}\right\} \tag{3.51}$$

at $x = x^+ \equiv \ln \bar{\kappa}R^+$ and $x = x^- \equiv \ln \bar{\kappa}R^-$.

For large wavenumbers n, $\phi(x)$ admits the asymptotic representation

$$\phi(x) = A\exp[n^j f_j(x)+\ldots+nf_1(x)+f_0(x)+n^{-1}f_{-1}(x)+\ldots]. \tag{3.52}$$

From (3.50) and the boundary conditions, grouping terms of the same power in n, we deduce that for $j>1$, $f_j(x)=0$ and for $j=1$, $f_1(x)$ satisfies

$$(\gamma\bar{h}-\sigma_1+\sigma_2)+2(\gamma\bar{h}-2h)\left(\frac{df_1}{dx}\right)^2+(\gamma\bar{h}+\sigma_1-\sigma_2)\left(\frac{df_1}{dx}\right)^4=0. \tag{3.53}$$

We shall show that the solution of (3.50) which satisfies the boundary conditions (3.51) for large values of n is

$$\phi(x) = A\exp[nf_{1a}(x)]+B\exp[nf_{1b}(x)], \tag{3.54}$$

where $f_{1a}(x)$ and $f_{1b}(x)$ are two solutions of (3.53). Without loss of generality we can

set

$$f_{1a}(x^-) = f_{1b}(x^-) = f_{0a}(x^-) = f_{0b}(x^-) = \ldots = 0.$$

For simplicity, the following notation is introduced:

$$\frac{df_{1a}(x^-)}{dx} = \rho_a, \qquad \frac{df_{1b}(x^-)}{dx} = \rho_b. \tag{3.55}$$

For $\phi(x)$ to be uniformly bounded for all n we must have $\mathrm{Re}\,(f_1(x)) < 0$, for which a sufficient condition is

$$\mathrm{Re}\left(\frac{df_1}{dx}\right) < 0. \tag{3.56}$$

When the entire plate is in the elliptic regime we can always find two non-trivial solutions of (3.53), f_{1a} and f_{1b}, with the property (3.56).

From the boundary condition (3.51) at $x = x^-$ and employing (3.54) and (3.55) we obtain

$$\left.\begin{aligned} (1+\rho_a^2)A + (\Gamma+\rho_b^2)B = 0, \\ [(\gamma\bar{h}-4h+\sigma_2)\rho_a + (\gamma\bar{h}-\sigma_2)\rho_a^3]A + [(\gamma\bar{h}-4h+\sigma_2)\rho_b \\ + (\gamma\bar{h}-\sigma_2)\rho_b^3]B = 0. \end{aligned}\right\} \tag{3.57}$$

The system (3.57) admits a non-trivial solution in A and B when its determinant vanishes, yielding

$$(\gamma\bar{h}-4h+\sigma_2)(1-\rho_a\rho_b) + (\gamma\bar{h}-\sigma_2)(\rho_a^2+\rho_b^2+\rho_a\rho_b+\rho_a^2\rho_b^2) = 0. \tag{3.58}$$

In view of (3.56), from (3.53) and (3.55) we get

$$\rho_a\rho_b = \sqrt{\frac{\gamma\bar{h}+\sigma_2}{\gamma\bar{h}-\sigma_2}}, \qquad \rho_a^2+\rho_b^2 = \frac{2(2h-\gamma\bar{h})}{\gamma\bar{h}-\sigma_2}, \tag{3.59}$$

and combining (3.58) with (3.59) we conclude

$$\sqrt{\frac{\gamma\bar{h}-\sigma_2}{\gamma\bar{h}+\sigma_2}} = 1-\frac{2h}{\sigma_2} \quad \text{at } r = R^-. \tag{3.60}$$

The boundary conditions (3.51) at the end $x = x^+$ are asymptotically satisfied since $\mathrm{Re}\,(f_1(x)) < 0$ so that for large n, ϕ and its derivatives tend to zero outside a vanishingly narrow zone near $x = x^-$.

The same analysis can be repeated starting with

$$f_{1a}(x^+) = f_{1b}(x^+) = f_{0a}(x^+) = f_{0b}(x^+) = \ldots = 0.$$

In this case the bifurcation mode is a surface one at $x = x^+$ and the critical condition is again (3.60) in which $\gamma\bar{h}$, h, and σ_2 are evaluated at $r = R^+$.

The critical condition (3.60) is identical with the critical condition given by YOUNG (1976) for the half-space problem. This result was expected since for a short wavelength surface mode, the curvature of the free surface does not affect the onset of a bifurcation instability and the plate behaves locally at the surface like a half-space.

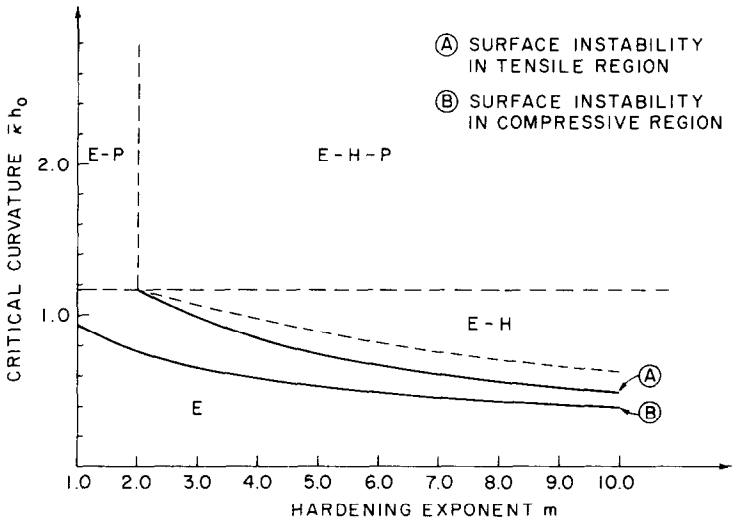

FIG. 4. Curves of the critical curvatures $\bar{\kappa} h_0$ corresponding to the onset of short wavelength surface instability vs hardening exponent m for the hypoelastic model. Also shown are regimes existing at a given curvature, for different values of the hardening exponent m.

In order to find the critical curvatures corresponding to the onset of surface instabilities in the case of the hypoelastic solid, (3.60), using also (2.8), (2.15), (3.14) and (3.19), gives

$$mx = 1 + mx\sqrt{\frac{1-2x}{1+2x}}, \tag{3.61}$$

where $x = \ln \bar{\kappa} R^+$ for $x > 0$ and $x = \ln \bar{\kappa} R^-$ for $x < 0$. Solving (3.61) we obtain one or two real roots according to whether the hardening exponent m is respectively smaller or bigger than 2. Figure 4 shows the critical curvature, corresponding to the short wavelength limit, as a function of the hardening exponent m. A surface instability in the compressive zone exists for all values of m, while a surface instability in the tensile zone occurs only for $m > 2$. Note that the bifurcation at the compressive region appears always before the one in the tensile region.

In the case of a hyperelastic material, (3.60) combined with (2.8), (2.15), (3.14) and (3.19) implies

$$\ln x\left(1 - \frac{1}{x^2}\right) = \frac{1}{m}, \tag{3.62}$$

where $x = \bar{\kappa} R^-$ for $x < 1$ and $x = \bar{\kappa} R^+$ for $x > 1$.

The results from (3.62) appear in Fig. 5. We emphasize that the instability in the compressive zone occurs before the one in the tensile zone. We also observe that for $m = 1$ (a neo-Hookean material) there is no surface instability in the tensile region. It can be verified that for both constitutive models employed, surface bifurcation instabilities always occur in the elliptic regime, as depicted in Figs 4 and 5.

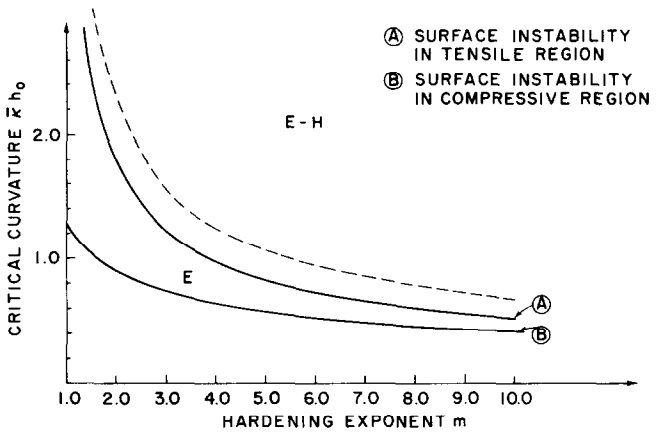

FIG. 5. Curves of the critical curvatures $\bar{\kappa}h_0$ corresponding to the onset of short wavelength surface instability vs hardening exponent m for the hyperelastic model. Also shown are regimes existing at a given curvature, for different values of the hardening exponent m.

4. NUMERICAL METHOD AND RESULTS

4.1 *Finite element method*

The lowest critical curvature of the plate is given by the minimum, over all integers n, of the lowest eigenvalues of each functional $F_n[\bar{\kappa}, \phi]$ in (3.27), where for $n \neq 0$, $\phi(r)$ is any arbitrary C^1 smooth function.

Because of the continuity requirements for ϕ, a convenient choice for element shape functions are the Hermitian cubics. Thus every element has two nodes, its endpoints, with two degrees of freedom per node, the values of ϕ and $d\phi/dr$ at this node. For the calculation of the element incremental stiffness matrix, four-point Gauss–Legendre quadrature is used. A modified Cholesky decomposition for the symmetric incremental stiffness matrix $[S]$ is performed, namely:

$$[S] = [L]^{\mathrm{T}}[D][L], \tag{4.1}$$

where $[L]$ is an upper triangular matrix with diagonal elements $L_{ii} = 1$ (no sum) and $[D]$ is purely diagonal. Bifurcation is possible when one element of $[D]$ vanishes.

For small wave numbers $n(h_0/l_0)$ the mesh is taken to be uniform, i.e. the interval $[R^-, R^+]$ is divided into equal subintervals. For large wave numbers, a surface boundary layer is observed, as anticipated from the asymptotic analysis given in the previous Section 3. Therefore, the mesh had to be refined at the ends.

More specifically, for $n(h_0/l_0) > 50$ a mesh refinement at the ends is necessary and the following transformation of coordinates was used:

$$\left|\frac{r_n - \frac{1}{2}(R^+ + R^-)}{\frac{1}{2}(R^+ - R^-)}\right| = 1 - \left[1 - \left|\frac{r_0 - \frac{1}{2}(R^+ + R^-)}{\frac{1}{2}(R^+ - R)}\right|\right]^{\delta}, \tag{4.2}$$

with r_n the new (refined) coordinates and r_0 the ones corresponding to the uniform mesh.

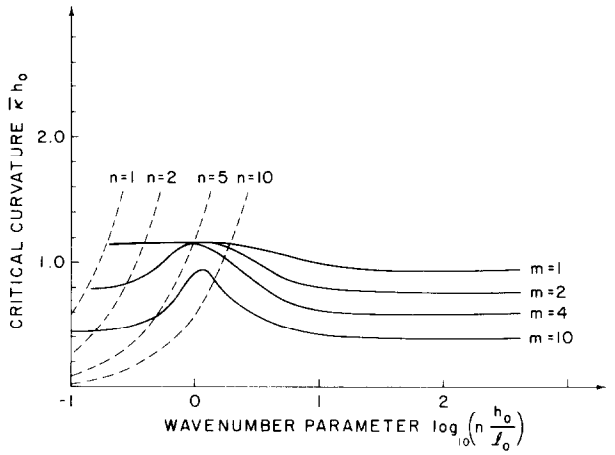

FIG. 6. Curves of the critical curvature $\bar{\kappa} h_0$ vs wavenumber parameter $n(h_0/l_0)$ for various values of the hardening exponent m, in the case of a hypoelastic material.

It is found that for $\delta = 2$ and 100 elements there is excellent agreement between the theoretically predicted critical curvature for the short wavelength limit and the numerical calculations for $n(h_0/l_0) > 100$.

All the numerical results presented here were obtained using 100 elements and a uniform mesh for $n(h_0/l_0) < 50$ or an r^2-type refinement at the ends of the interval $[R^-, R^+]$ for $n(h_0/l_0) > 50$. Some of the calculations were repeated for 200 elements and gave critical curvatures which agreed at least to four digits with the results obtained when 100 elements were used.

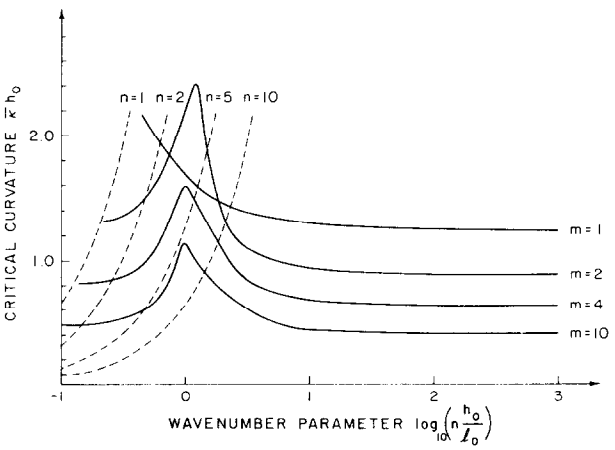

Fig. 7. Curves of the critical curvature $\bar{\kappa} h_0$ vs wavenumber parameter $n(h_0/l_0)$ for various values of the hardening exponent m in the case of a hyperelastic material.

4.2 *Numerical results*

Figures 6 and 7 illustrate the dependence of the critical curvature, $\bar{\kappa}h_0$, on the wavenumber parameter, $n(h_0/l_0)$, for the hypoelastic and the hyperelastic constitutive models respectively. Results are displayed for four values of the strain-hardening exponent $m = 1, 2, 4, 10$. In each case, the initial yield strain ε_y is taken to be 0·002. An upper limit to the curvature achievable by pure bending is set by the obvious requirement that the plate cannot be bent through an angle exceeding 360°. In a curvature vs wavenumber parameter diagram, the line separating the admissible from the non-admissible region obeys the equation

$$\bar{\kappa}h_0 = \left(n\frac{h_0}{l_0}\right)\frac{2\pi}{n}. \tag{4.3}$$

Curves satisfying (4.3) are drawn in a broken line for values of the wavenumber $n = 1, 2, 5, 10$ in Figs 6 and 7.

As it can be seen in Figs 6 and 7, for all cases considered, the smallest critical curvature corresponds to a surface instability in the compressed zone of the plate. Two remarks concerning the lowest critical curvature follow from the above observation. First, since the yield strain ε_y does not enter the equations for the short wavelength mode (3.61) and (3.62), the lowest critical curvature is independent of ε_y. Second, since the onset of a surface bifurcation instability is not sensitive to the boundary conditions of the two end-sections of the plate, we may conjecture that the lower critical curvature is independent of the exact form of the boundary conditions at the two straight ends of the plate, presuming that the equations of the boundary value problem corresponding to the new set of boundary conditions are still self-adjoint.

The fact that the first bifurcation occurs when the entire plate is in the elliptic regime was expected in view of the proposition in Section 3.2. A similar phenomenon has been observed by BASSANI, DURBAN and HUTCHINSON (1979). In their recent analysis of a pressurized spherical cavity, in an infinite elastic–plastic medium, they found that a short wavelength surface mode is the first bifurcation mode encountered in the deformation history.

For a given uniaxial stress–strain curve and a given wavenumber parameter, the curvature at bifurcation is always higher for the hyperelastic model, because of its higher incremental shear modulus. The difference between the critical curvatures predicted by the two theories, for the same wavenumber parameter and uniaxial stress–strain behavior, decreases with increasing hardening exponent, since bifurcation occurs at smaller strains. It can be seen in Figs 6 and 7 that for $m = 10$ the corresponding curves of $\bar{\kappa}h_0$ vs $n(h_0/l_0)$ are almost identical.

The critical curvature is, in most cases, an increasing function of the hardening exponent when the wavenumber parameter and the yield strain of the material are held fixed. One exception seems to be in the case of a hyperelastic material (Fig. 7) where near $n(h_0/l_0) = 1$ the critical curvatures for $m = 2$ are higher than the ones for $m = 1$.

The solid line in Fig. 8 depicts the curvature corresponding to the maximum moment $(\bar{\kappa}h_0)_{max}$ as a function of the hardening exponent m for an initial yield strain

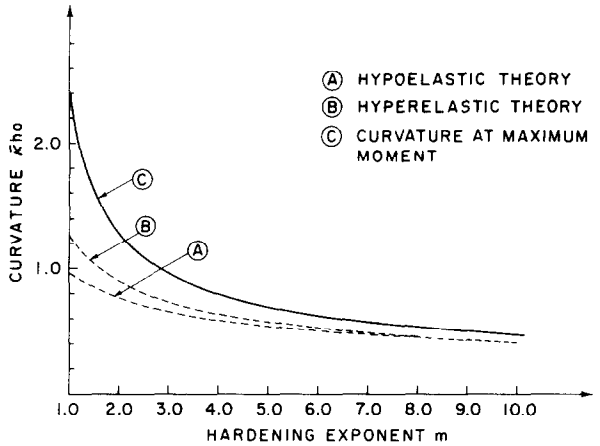

FIG. 8. Curves of the curvature $\bar{\kappa}h_0$ corresponding to maximum moment (solid line) and to short wavelength notes (broken lines) as a function of the hardening exponent m.

$\varepsilon_y = 0{\cdot}002$. The two broken lines in Fig. 8 show the critical curvature at the onset of a surface bifurcation instability in the compressed zone for the hypoelastic and the hyperelastic body and are copied from Figs 4 and 5 respectively, for comparison purposes.

As we can see from Fig. 8 the short wavelength mode in the compressed zone always occurs before the plate attains its maximum moment. The distance between the curvature corresponding to the maximum moment and the critical curvature for the surface mode in the compressed region decreases monotonically with increasing hardening exponent.

The dependence of the critical curvature $\bar{\kappa}h_0$ on the wavenumber parameter $n(h_0/l_0)$ is not necessarily monotonic. For $m > 2$ in the hypoelastic model and $m > 1$

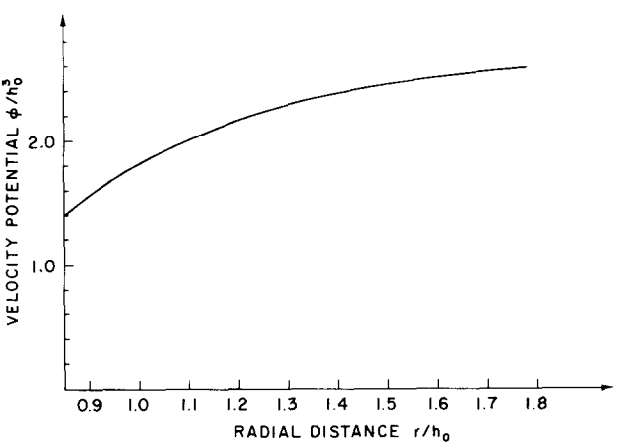

FIG. 9. Long wavelength $[n(h_0/l_0) = 0{\cdot}2]$ eigenmode $\phi(r)/h_0^3$ vs radial distance r/h_0 for a hypoelastic material with $m = 4$ (the corresponding critical curvature is $\bar{\kappa}h_0 = 0{\cdot}8199$).

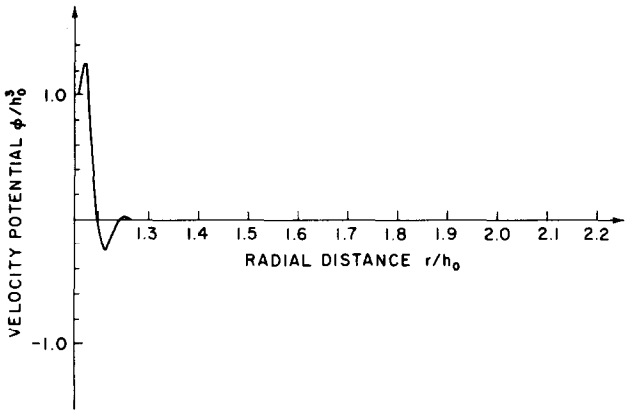

FIG. 10. Short wavelength $[n(h_0/l_0) = 10]$ eigenmode $\phi(r)/h_0^3$ vs radial distance r/h_0 for a hypoelastic material with $m = 4$ (the corresponding critical curvature is $\bar{\kappa}h_0 = 0{\cdot}6379$).

in the hyperelastic one, we observe that relatively long wavelength modes are available at curvatures only slightly above the ones corresponding to the maximum moment. All the non-monotonic $(\bar{\kappa}h_0)$-curves present a peak at the vicinity of the "square pattern" mode, i.e. when $n(h_0/l_0) = 1$.

Figure 9 depicts the eigenmode $\phi(r)/h_0^3$ as a function of the radial distance r/h_0 for a hypoelastic material with hardening exponent $m = 4$ and yield strain $\varepsilon_y = 0{\cdot}002$ at a wavenumber parameter $n(h_0/l_0) = 0{\cdot}2$. The eigenmode in this case varies very smoothly with the distance. Figure 10 depicts the eigenmode $\phi(r)/h_0^3$ as a function of the radial distance r/h_0 for the same material at a wavenumber $n(h_0/l_0) = 10$. In this case we observe a boundary layer effect in the eigenmode which practically vanishes at a distance of order 1/10 of the inner radius away from the surface.

Some of the numerical calculations were repeated for a yield strain $\varepsilon_y = 0{\cdot}01$ but no significant difference in the results was observed.

5. Concluding Remarks

As explained in the Introduction, the physical problem that we have tried to model in this work is the following: *Given a plate with initial length* l_0 *and thickness* h_0, *what is the maximum curvature achievable in a pure bending process*?

One limit is a purely geometrical one. The plate cannot be bent through an angle exceeding 360°. The corresponding limiting curvature is

$$(\bar{\kappa}h_0)_{\text{lim}} = 2\pi \frac{h_0}{l_0}. \tag{5.1}$$

The other, denoted by $(\bar{\kappa}h_0)_{\text{cr}}$, depends only on material properties and corresponds to failure due to the onset of a surface bifurcation instability in the compressed zone, is given by (3.61) and (3.62). It follows from (5.1) that a bifurcation instability occurs

prior to the plate being bent through an angle of 360° when

$$\frac{(\bar{\kappa}h_0)_{\text{lim}}}{2\pi} = \frac{h_0}{l_0} \geqslant \frac{(\bar{\kappa}h_0)_{\text{cr}}}{2\pi}. \tag{5.2}$$

If (5.2) is not satisfied, the plate is bent through a complete circle before any bifurcation occurs. For example, for a hyperelastic material with hardening exponent $m = 1$ bifurcation instability will occur prior to the ends of the plate touching in plates with $h_0/l_0 \geqslant 0{\cdot}203$ while for $m = 10$ a bifurcation instability occurs prior to touching in a hypoelastic or hyperelastic plate when $h_0/l_0 \geqslant 0{\cdot}064$.

If bifurcation occurs before the plate is bent through a complete circle, the corresponding critical angle formed by the plate at the onset of the instability is

$$\theta_{\text{cr}} = (\bar{\kappa}h_0)_{\text{cr}} \frac{l_0}{h_0}. \tag{5.3}$$

Thus, for example, instability occurs in a hypoelastic plate with initial dimensions $h_0/l_0 = 0{\cdot}1$ at an angle $\theta_{\text{cr}} = 5{\cdot}96$ rad (341·5°) for $m = 4$ and at an angle of $\theta_{\text{cr}} = 4{\cdot}06$ rad (232·6°) for $m = 10$. One can also ask what are the initial dimensions required for a plate to be bent through a given angle without encountering a bifurcation. For example, to achieve a final angle of 180° in a hypoelastic or hyperelastic plate with $m = 10$, the initial dimensions of the plate must satisfy $h_0/l_0 > 0{\cdot}129$.

The analysis carried out in this work shows that bifurcation instability can be observed in a plate under pure bending once the curvature exceeds a certain limit which is an increasing function of the hardening exponent of the material, provided, of course, that the initial dimensions of the plate satisfy (5.2).

These critical curvatures are high even for relatively low hardening materials. The influence of imperfections as well as the consideration of more appropriate plastic constitutive models on the critical curvature merits further investigation.

ACKNOWLEDGEMENTS

The author wishes to extend his sincere appreciation to his advisor Professor A. NEEDLEMAN for his help and encouragement during the course of this work. Helpful discussions with Professors C. DAFERMOS and A. C. PIPKIN (Division of Applied Mathematics, Brown University) are also gratefully acknowledged. This work was supported by the U.S. National Science Foundation under Grant No. ENG 76–16421.

REFERENCES

BASSANI, J. L., DURBAN, D. and HUTCHINSON, J. W. 1979 *Proc. Camb. phil. Soc.* **87**, p. 339.

BIOT, M. A. 1965 *Mechanics of Incremental Deformation*, p. 194. Wiley, New York.

GREEN, A. E. and ZERNA, W. 1954 *Theoretical Elasticity*, p. 108. Oxford University Press.

HECKER, S. S.	1976	*Constitutive Equations in Viscoplasticity: Computational and Engineering Aspects. AMD* **20,** *ASME*, New York.
HILBERT, D. and COURANT, R.	1953	*Methods of Mathematical Physics*, Vol. 2, p. 577. Interscience, New York.
HILL, R.	1957	*J. Mech. Phys. Solids* **5,** 229.
	1967	*Ibid.* **15,** 79.
	1969	*Problems in Mechanics: Deformation of Solid Bodies* (in Russian), (Novozhilov 60th Anniversary Volume), (edited by L. I. Sedov), p. 459. Academy of Sciences, S.S.S.R., University of Leningrad.
HILL, R. and HUTCHINSON, J. W.	1975	*J. Mech. Phys. Solids* **23,** 239.
HUTCHINSON, J. W.	1970	*Proc. R. Soc. Lond.* A**319,** 247.
	1974	*Advances in Applied Mechanics*, Vol. 14, p. 67. Academic Press, New York.
LIN, T. H.	1971	*Ibid.* Vol. 11, p. 255. Academic Press, New York.
RICE, J. R.	1976	*Proceedings of the 14th International Congress of Theoretical and Applied Mechanics* (Delft, 30 August–4 September 1976), (edited by W. T. Koiter), Vol. 1, p. 207. North-Holland, Amsterdam.
RIVLIN, R. S.	1950	*Phil. Trans. Roy. Soc. Lond.* A**242,** 173.
STÖREN, S. and RICE, J. R.	1975	*J. Mech. Phys. Solids* **23,** 421.
VAN HOVE, L.	1947	*Proc. Kon. Ned. Acad. Wetensch.* **50,** 18.
YOUNG, N. J. B.	1976	*J. Mech. Phys. Solids* **24,** 77.